

Important role of collective cell migration and nerve fiber density in the development of deep nodular endometriosis

Renan Orellana, Ph.D.,^a Javier García-Solares, M.Sc.,^a Jacques Donnez, M.D., Ph.D.,^c Olivier van Kerk, B.Sc.,^a Marie-Madeleine Dolmans, M.D., Ph.D.,^{a,b} and Olivier Donnez, M.D., Ph.D.^d

^a Pôle de Gynécologie, Institut de Recherche Expérimentale, Université Catholique de Louvain, Brussels, Belgium;

^b Gynecology Department, Cliniques Universitaires Saint Luc, Brussels, Belgium; ^c Société de Recherche pour l'Infertilité, Brussels, Belgium; and ^d Institut du Sein et de Chirurgie Gynécologique d'Avignon, Polyclinique Urbain V (ELSAN Group), Avignon, France

Objective: To evaluate deep nodular endometriotic lesions induced in baboons over 12 months and analyze collective cell migration and nerve fiber density.

Design: Morphologic and immunohistochemical analysis of endometriotic lesions induced in baboons over the course of 1 year.

Setting: Academic research unit.

Animal(s): Three female baboons (*Papio anubis*).

Intervention(s): Recovery of induced deep nodular endometriotic nodules from baboons.

Main Outcome Measure(s): Evaluation of the morphology of glands by analysis of the center of lesions and the invasion front; immunohistochemical staining with Ki67, E-cadherin, and β -catenin for investigation of mitotic activity and cell-cell junctions, and with protein gene product 9.5 and nerve growth factor (NGF) for study of nerve fiber density (NFD).

Result(s): All (100%) of the lesions were invasive 1 year after induction, compared with 42.29% after 6 months. Glands from the invasion front showed significantly reduced thickness but significantly higher mitotic activity. E-Cadherin and β -catenin expression were similar between the center and front. NFD was significantly higher in lesions induced after 1 year than after 6 months, and NGF expression was significantly lower in 1-year lesions than in 6-month lesions.

Conclusion(s): Nodular endometriotic lesions induced in the baboon model were found to be significantly more invasive and innervated after 12 months than after 6 months. The invasive phenotype was highly expressed in glands at the invasion front, and our study suggests that nerve fibers play a role in the development of lesions as observed in women. (Fertil Steril® 2017;107:987–95. ©2017 by American Society for Reproductive Medicine.)

Key Words: Deep nodular endometriosis, baboon model, collective cell migration, nerve fibers, nerve fiber density, invasion

Discuss: You can discuss this article with its authors and with other ASRM members at <https://www.fertstertdialog.com/users/16110-fertility-and-sterility/posts/14271-23263>

Endometriosis is one of the most frequently encountered benign gynecological diseases, known to occur in 7%–10% of women of

reproductive age (1, 2). It is now well established that three different forms of endometriosis can occur in the pelvis: peritoneal endometriosis, ovarian

endometriosis, and deep endometriotic nodules of the rectovaginal septum (3). Most deep lesions originate from the posterior part of the cervix and secondarily infiltrate the anterior wall of the rectum (4, 5). Anaf et al. were the first to pinpoint a close histologic relationship between nerves and endometriotic foci, and between nerves and the fibrotic component of nodules (6). The pathogenesis of these endometriotic nodules (whose histology reveals typical features of adenomyosis with smooth muscle hyperplasia and fibrosis) remains unclear and probably

Received October 18, 2016; revised December 21, 2016; accepted January 13, 2017; published online February 24, 2017.

R.O. has nothing to disclose. J.G.-S. has nothing to disclose. J.D. reports grants and personal fees from Gedeon Richter Group and is a member of the *Fertility and Sterility* Editorial Board. O.v.K. has nothing to disclose. M.-M.D. has nothing to disclose. O.D. has nothing to disclose.

R.O. and J.G.-S. should be considered similar in author order.

Supported by the Fonds National de la Recherche Scientifique de Belgique (grant no. 5/4/150/5 to M.M.D.).

Reprint requests: Marie-Madeleine Dolmans, M.D., Ph.D., Institut de Recherche Expérimentale et Clinique, Université Catholique de Louvain, Avenue Mounier 52, bte B1.52.02, Brussels B-1200, Belgium (E-mail: marie-madeleine.dolmans@uclouvain.be).

Fertility and Sterility® Vol. 107, No. 4, April 2017 0015-0282/\$36.00

Copyright ©2017 American Society for Reproductive Medicine, Published by Elsevier Inc.

<http://dx.doi.org/10.1016/j.fertnstert.2017.01.005>

differs from the pathogenesis of peritoneal and ovarian endometriosis (3).

Some authors have reported high rates of spontaneous and induced peritoneal endometriosis in baboons (7, 8), but we found only 4.8% and 20.7% of spontaneous and induced endometriosis, respectively, with the use of the same method, suggesting that baboons are able to cleanse and renew their peritoneum (9). Based on our previous observational studies of iatrogenic adenomyosis in humans (10, 11), we developed the first nonhuman animal model for nodular endometriosis (12). Although grafting endometrium or myometrium alone did not induce any endometriosis at all, when endometrium was associated with submyometrial layers, including the junctional zone (JZ), we observed a 100% rate of endometriosis induction, highlighting the importance of the JZ in the development of nodular endometriosis in this model. Nerve growth factor (NGF) expression was significantly higher in invasive lesions than in noninvasive lesions, but nerve fiber density (NFD) was similar in both groups (13). We also found altered morphology, increased mitotic activity, and fewer adhesion molecules in invasive glands present in induced nodular endometriosis, particularly along the invasion front, suggesting that collective cell migration is involved in the invasion process of deep endometriotic lesions induced in a baboon model (14).

The goal of the present study was to determine if nerves still grow in invasive and noninvasive lesions >6 months after grafting and to evaluate the role of the lesion environment in neuroregeneration. We explored the kinetic factors by analyzing collective cell migration and innervation in nodular endometriotic lesions induced after 12 months compared with 6 months (12, 13) and investigated morphology, mitotic activity, expression of adhesion molecules, NFD, and NGF. Because invasion was observed mainly in the bowel and cervix in our previous studies (12–14), we decided to focus on retroperitoneal pelvic areas close to the ureters.

MATERIALS AND METHODS

Extrapolating from previous studies (12), we estimated that we could obtain 15 induced nodular endometriosis specimens with the use of only three baboons by grafting fragments containing the JZ. This allowed us to reduce the number of animals, in line with the principles of ethical conduct in animal research, as well as reducing overall costs. Three female baboons (*Papio anubis*) were studied at the Institute of Primate Research (IPR), Nairobi, Kenya. Approval was obtained from the Institutional Scientific Evaluation and Review Committee and the Animal Care and Use Committee of the IPR. All of the baboons tested negative for common pathogens (bacterial and viral infections as well as parasites) and were screened for tuberculosis, simian T-lymphotropic virus 1, and simian immunodeficiency virus. The animals were housed in single cages and fed commercial monkey pellets (Gold Star Products) and seasonal fruit and vegetables with free access to water. A comparison was made with lesions identified in previous studies (13, 14), where deep endometriotic nodules were induced in ten baboons and recovered 6 months later.

Induction of Deep Nodular Endometriosis

The baboons initially underwent median laparotomy. After complete pelvic and abdominal exploration, no spontaneous endometriosis was found in any of the three animals. Bilateral salpingo-oophorectomy was performed to avoid individual variations in hormone secretion, and hormone replacement therapy was initiated on the same day (E₂ valerate, 2 mg/d orally; Progynova; Bayer Schering Pharma Berlin). Hormone replacement therapy was administered daily with food under the supervision of a designated technician and controlled by a veterinarian. Uterine biopsies were obtained by means of a cold knife.

Biopsies of 1 cm³ containing endometrium and myometrium were grafted beneath the peritoneum in five different sites in the pelvic area: upper and lower parts of both uterosacral ligaments close to the ureters (n = 4) and rectovaginal septum (n = 1). The grafting process involved opening the peritoneum with cold scissors, placing the biopsies in the relevant sites, and then closing the peritoneum by means of simple suture with the use of absorbable 3/0 Vicryl FS2 (Johnson and Johnson). The biopsy itself was not sutured in any case. When uterine biopsies were placed close to the ureters on both sides, it is important to note that ureterolysis was not performed, because we did not want to facilitate invasion of the ureters. After 1 year, laparotomy was performed to recover the lesions. All induced lesions were identified and photographed before complete excision, then measured, fixed in formalin, and embedded in paraffin. All sections were assessed by two investigators (O.D. and R.O.) blinded to lesion phenotypes. Fifty to 200 consecutive serial sections of each lesion were evaluated up to the invasion front. Histologic analysis was performed over the entire lesion and where glandular density was most concentrated. All sections were scanned with the use of the Leica SCN400 scanner (Leica Biosystems Wetzlar), and image acquisition was achieved with the use of the Tissue IA system (Leica Biosystems Dublin). Image J software was applied for morphologic analysis and immunohistochemical quantification, using the color deconvolution plugin to isolate the diaminobenzidine (DAB) channel.

Morphologic Analysis

The total size of each lesion was determined immediately after its extraction by measuring three dimensions in the corresponding x, y, and z axes. Hematoxylin-eosin staining was carried out for microscopic analysis of the lesions: surface area (mm²), glandular density (glands/mm²), and surrounding organ invasion. In line with our previous publications (12, 13), invasion was defined as the presence of glands and stroma inside surrounding organs, as detected with the use of serial sections (50–200 sections). In invasive lesions, a morphologic distinction was made between the center of the lesion (trailing edge) and the invasion front (leading edge). Well circumscribed lesions were classified as noninvasive lesions. Gland thickness was calculated by measuring the distance between the external (basal) and internal (apical) parts of the gland. To avoid artifacts due to sectioning, we excluded glands without a lumen and areas with multilayer cells.

Immunohistochemical Analysis

Mitotic activity was assessed by means of Ki67 immunohistochemical staining and counting of Ki67-positive nuclei per gland (proliferation index) in the defined phenotypes of whole lesions and areas. Briefly, deparaffinization was performed with the use of X-Solv paraffin-clearing solvent (Yvsolab) followed by a permeabilization step with Tris-buffered saline solution and Triton 0.1%. Endogenous peroxidase activity quenching, heat epitope retrieval, and blocking of nonspecific staining were all carried out. Thereafter, Ki67 monoclonal antibody (1:50, Dako M7240) was incubated overnight at 4°C, before incubation with secondary antibody (1:2, B17 Dako K4001 Envision anti-mouse). Labeling was done with use of the DAB substrate kit (Vector Laboratories) according to the manufacturer's instructions. Baboon bowel mucosa was used as a positive control sample for Ki67, showing strong nuclear staining in proliferative goblet cells of the intestinal epithelium (Supplemental Fig. 1; Supplemental Figs. 1–5 are available online at www.fertstert.org). Negative control samples were processed by omitting the primary antibody, and no staining was detected (Supplemental Fig. 1). Immunostaining of β -catenin (1:300, Beckton Dickinson BDB610153) and E-cadherin (1:500, Dako M3612) antibodies also involved deparaffinization, antibody incubation, and labeling, achieved with the use of the Benchmark XT IHC/ISH module (Ventana-Roche).

For preparation of the slides, EDTA-borate alkaline buffer was applied (60 minutes for β -catenin and 30 minutes for E-cadherin) before incubation with blocking solution (30 minutes for β -catenin and 12 minutes for E-cadherin). Levels of E-cadherin and β -catenin were determined by means of a score obtained with the use of a freehand selection tool measuring DAB-positive pixels and the area of glands, excluding the lumen. Eutopic endometrium from the baboons was used as a positive control sample for E-cadherin and β -catenin, showing strong expression in the membrane of epithelial cells (Supplemental Fig. 1) but no staining in the absence of the primary antibody (Supplemental Fig. 1). For protein gene product (PGP) 9.5 and NGF, immunohistochemistry and quantification were performed as previously reported (8) with the use of rabbit polyclonal anti-human PGP9.5 (1:1,000; Dako Glostrup) and anti-human NGF (1:3,000; Santa Cruz Biotechnology) as primary antibodies, before incubation with the secondary antibody (Envision; Dako Glostrup). Baboon intestinal tissue was used as a positive control for PGP9.5 and NGF immunostaining, but no expression was detected in the absence of the primary antibody (Supplemental Fig. 1). NFD was calculated by counting the number of PGP9.5-positive fibers per area of tissue (mm^2), and NGF scores were obtained based on the number of positive pixels covering the area.

To compare 6-month and 12-month lesions, two procedures were carried out to avoid technical mismatches between the groups. First, 6-month lesions (previously analyzed with the use of the Mirax Midi scanner) were once again scanned in the same device as used for 12-month lesions, and the new values obtained showed the same significant differences as previously reported (data not shown). Second, NFD and

NGF scores were normalized with the use of values obtained from corresponding eutopic tissue.

The Mann-Whitney test was used for statistical analysis (Graphpad Prism 6 software) and Pearson correlation test for comparison of groups and gland analysis. A value of $P < .05$ was considered to be statistically significant.

RESULTS

Macroscopic Analysis

A total of 15 endometriotic lesions (100% induction rate; Supplemental Fig. 2) were recovered from the three baboons. They showed a macroscopically nodular aspect and hard consistency (Fig. 1A and 1B), with a mean volume of $531.15 \pm 389.28 \text{ mm}^3$ (Supplemental Fig. 2). The mean surface area of the largest section was $32.50 \pm 21.81 \text{ mm}^2$. All lesions induced 1 year after grafting exhibited glands in surrounding organs, at a density of $2.48 \pm 2.05 \text{ glands/mm}^2$; therefore they were classified as invasive in 100% of cases (Supplemental Fig. 2). The invasion front was identified in surrounding connective tissue in all samples ($n = 15/15$ lesions; Fig. 1C), with clear connections to the lesion center visible on serial sections. In lesions induced close to the ureters, glands from the invasion front were mainly found in the muscularis of the ureter ($n = 12/12$), and even reaching the ureteral epithelium ($n = 1/12$ lesions; Fig. 1D). Cervical muscularis invasion was also observed ($n = 1/3$ lesions) when biopsies were grafted to the rectovaginal septum. Glands present at the invasion front showed significantly lower wall thickness values ($13.79 \pm 5.6 \mu\text{m}$; $P < .001$; Fig. 2A) than those in the center ($29.84 \pm 9.80 \mu\text{m}$; Fig. 2A).

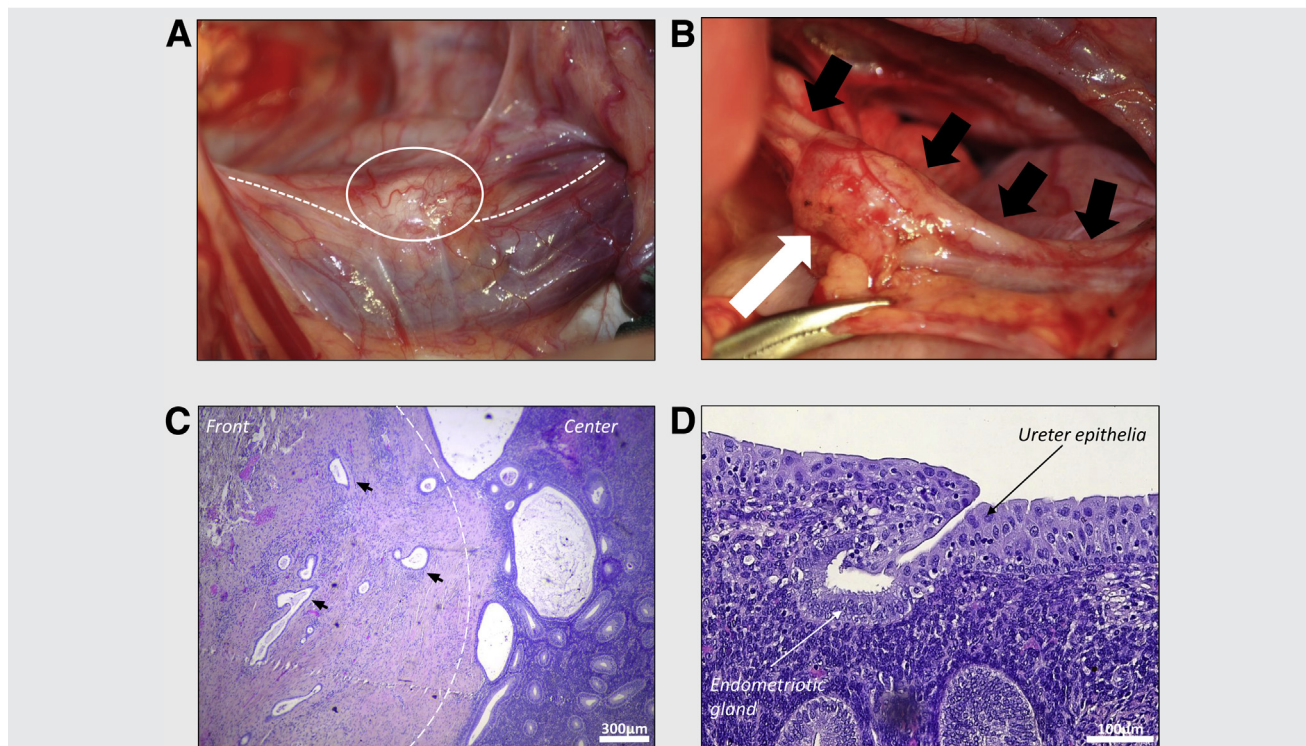
Mitotic Activity

Ki67 staining was found to be significantly more extensive at the invasion front ($3.03 \pm 2.2 \times 10^{-4}$ nuclei/surface area; $P < .001$; Fig. 2B) than in the center ($0.42 \pm 0.82 \times 10^{-4}$ nuclei/surface area; Fig. 2B) of lesions. No significant inter-variability was observed between baboons or grafting sites (data not shown).

We encountered a significant correlation between gland thickness and mitotic activity ($P < .001$; $r^2 = 0.36$) when all glands were taken into account (Supplemental Fig. 3), indicating that the thinner the glands, the higher their mitotic activity. Glands in the center of invasive lesions demonstrated a significant correlation ($P = .00185$; $r^2 = 0.08242$), whereas those at the invasion front did not ($P > .05$; $r^2 = 0.07262$).

We noted that Ki67 staining showed heterogeneous distribution among lesions. Glands located in the outermost areas of the center, thus close to the invasion front, exhibited greater mitotic activity than glands in the center ($P < .001$; Supplemental Fig. 4A and 4B). An analysis of lesions comparing glands in peripheral areas of the center (outer) with those in central areas of the center (inner) of invasive lesions revealed that outer glands showed higher mitotic activity ($17.86 \pm 16.60 \times 10^4$ nuclei/surface area; $P < .001$; Supplemental Fig. 4C) and lower wall thickness ($19.98 \pm 5.34 \mu\text{m}$; Supplemental Fig. 4B) values than inner glands

FIGURE 1



Analysis of baboon endometriotic lesions 1 year after induction. (A) Macroscopic view of a nodular endometriotic lesion in the center of the *white circle*, with the ureter indicated by a *dotted white line*. (B) Macroscopic view of the lesion after opening the retroperitoneum. The induced nodular endometriotic lesion (*white arrow*) shows dense adhesions with the ureter (*black arrows*). (C) Microscopic analysis of an invasive lesion, hematoxylin-eosin staining. Invasive glands (*arrows*) can be seen migrating out of the center of the lesion, delimited by a *dotted white line*. (D) Microscopic analysis of an endometriotic gland (*white arrow*) infiltrating the ureteral muscularis and mucosa and fusing with the urothelium (*black arrow*).

Orellana. Endometriosis: innervation and invasion. *Fertil Steril* 2017.

($0.22 \pm 0.50 \times 10^4$ nuclei/surface area and $29.79 \pm 7.06 \mu\text{m}$, respectively; $P < .001$).

Adhesion Molecules

Expression levels of β -catenin were similar between the center (155.7 ± 28.5 pixels/surface area) and the front (145.7 ± 28.2 pixels/surface area; Fig. 3A). Staining was identified only in glands, and was limited to the membrane in contact with neighboring glandular cells. Analysis of E-cadherin levels showed no difference between glands in the lesion center (71.82 ± 32.31 pixels/surface area) and those at the invasion front (73.88 ± 25.09 pixels/surface area; Fig. 3B).

PGP9.5 and NGF Detection

NFD was evaluated by means of PGP9.5 immunostaining, with lesions exhibiting a significantly higher density (7.87 ± 2.74 PGP9.5/ mm^2) than eutopic endometrium (4.29 ± 0.90 PGP9.5/ mm^2 ; $P = .0364$, Fig. 4A). Nerves were found to be more abundant in lesions than in their surrounding periphery (2.41 ± 0.77 PGP9.5/ mm^2 ; $P < .001$; Supplemental Fig. 5A). NGF staining of glandular epithelial cells of lesions was significantly less extensive in endometriotic lesions

(1.103 ± 0.13 NGF score) than in eutopic tissue (1.783 ± 0.80 NGF score, $P = .0328$; Fig. 4B). However, no difference was observed in stromal cell expression of NGF between lesions and eutopic endometrium (1.75 ± 0.48 vs. 2.11 ± 0.32 NGF score; $P = .178$; Supplemental Fig. 5C). Significantly higher NFD and significantly lower NGF expression levels were observed in nodular lesions induced after 12 months than after 6 months (Supplemental Figs. 4B and 5D; $P < .001$).

DISCUSSION

During the past two decades, the prevalence of deep nodular endometriosis has clearly increased, but its pathophysiology remains a subject of debate (15). We successfully developed the first experimental induction model of deep nodular endometriosis in baboons (*Papio anubis*), obtaining a 100% induction rate with subsequent invasion of surrounding organs in 42% of lesions (12). These lesions were classified as invasive because they showed endometriotic glands and stroma invading surrounding organs. Morphologic analysis and immunohistochemistry pointed to the existence of a clear invasive phenotype, characterized by thin glands with low levels of adhesion molecules and high mitotic activity (14). By grafting endometrium together with myometrium

FIGURE 2

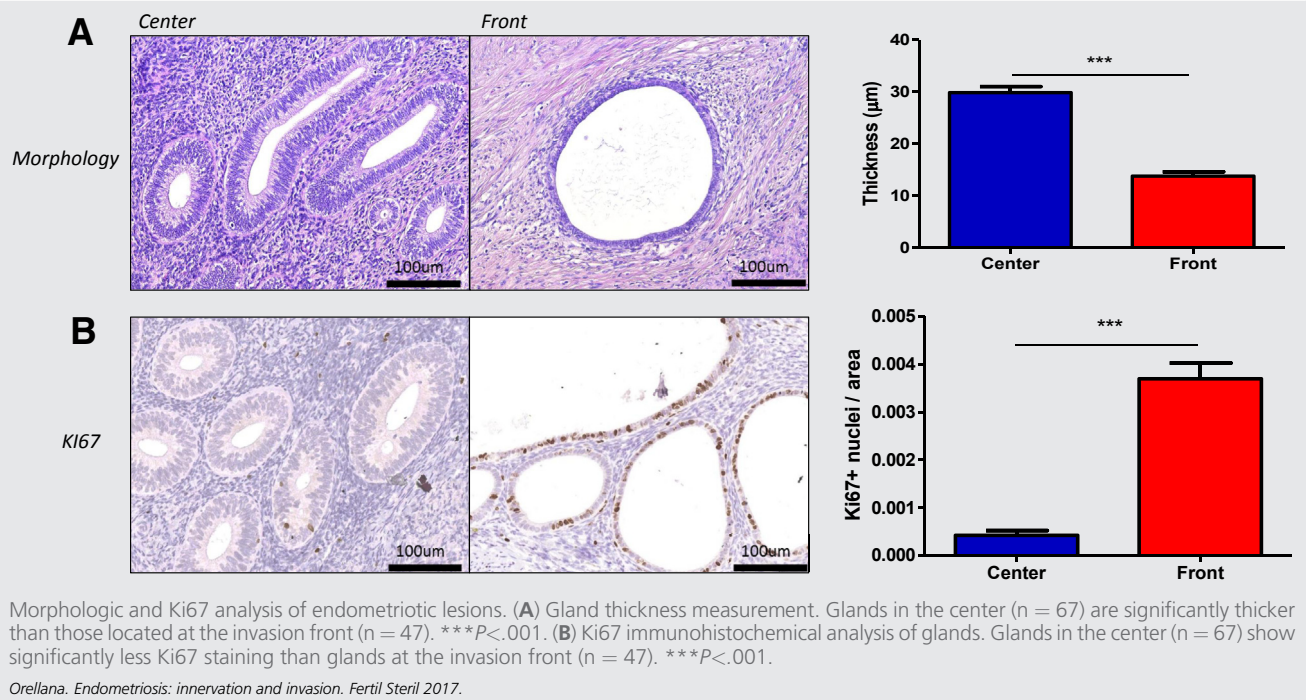


FIGURE 3

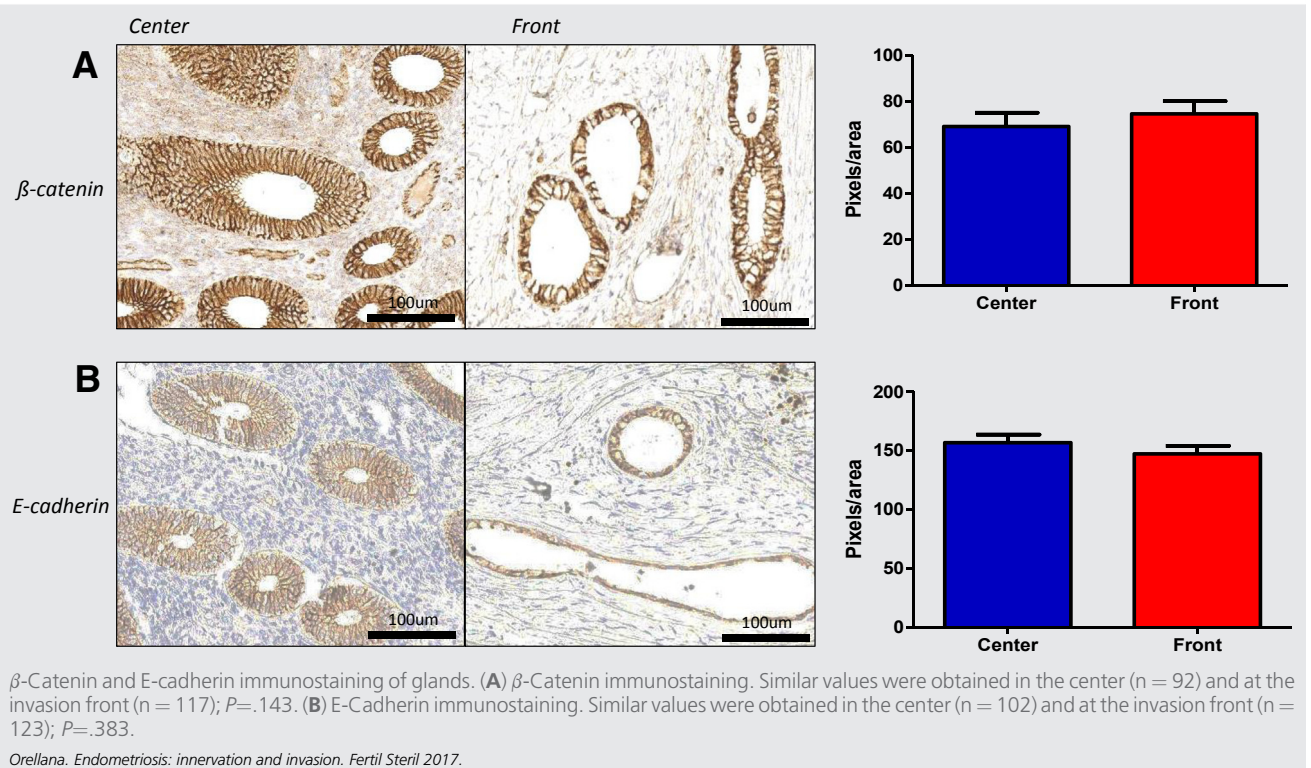
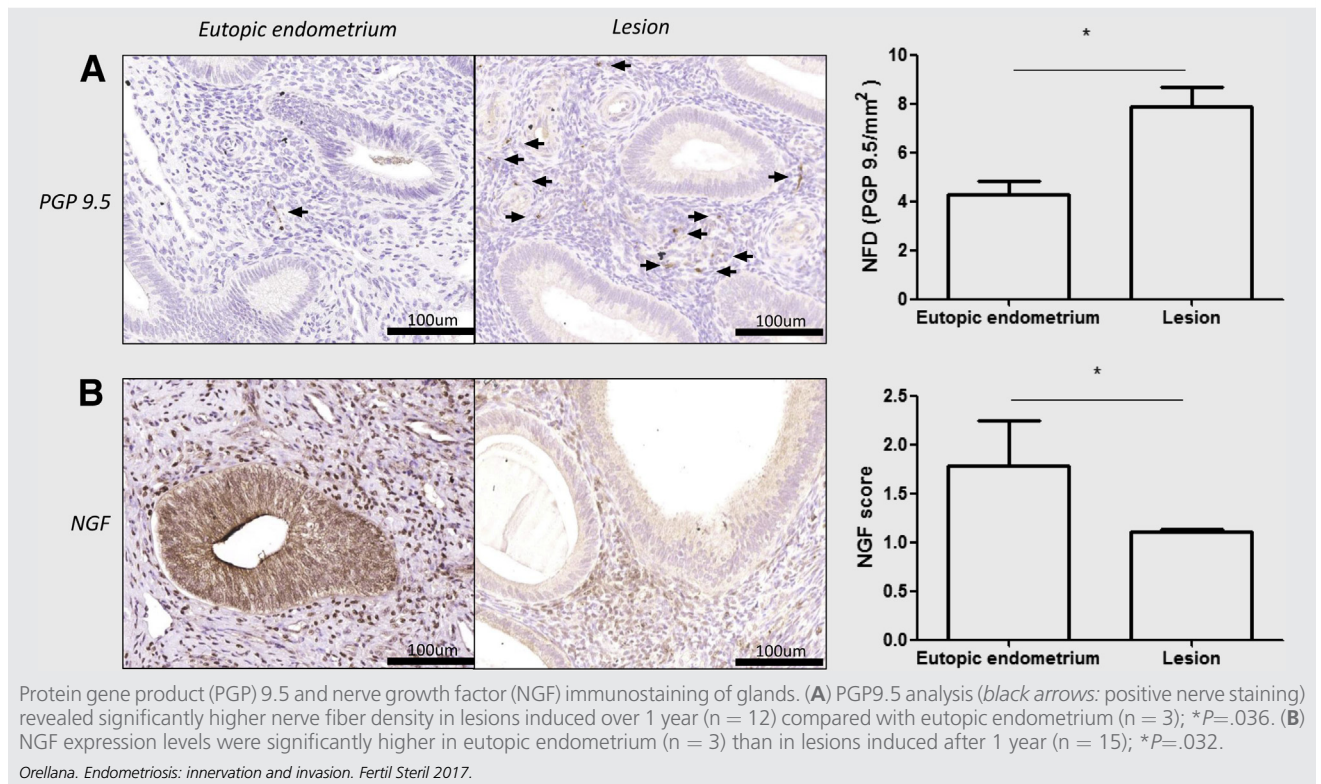


FIGURE 4



(containing the JZ), we were able to induce endometriotic lesions similar to those observed in women with deep nodular lesions (12). The presence of the JZ in specimens was fundamental to lesion development (12, 13). The JZ is also required for development of uterine adenomyosis (16), indicating a possible common origin with deep nodular endometriosis.

The presence of noninvasive lesions containing glands with an invasive phenotype implies that these induced lesions could become invasive over time, which is why we chose to analyze deep nodular lesions induced after 12 months.

Morphologic Comparison with Lesions Induced after 6 Months

An invasive phenotype was observed in 100% of lesions after 1 year, which is significantly different ($P < .001$) from the 42% observed at 6 months. This strongly suggests that the invasive potential of lesions increases over time, and that some noninvasive lesions at 6 months could exhibit an invasive phenotype 1 year after induction. It sheds light on the developmental process, demonstrating that these glands may be able not only to evolve with time, but also to migrate out of and invade surrounding organs.

In the present study, a high mitotic index was significantly associated with thin glands. This corroborates the idea of acquisition of an invasive phenotype with time that could cause these glands to migrate out of the center and become part of the invasion front.

These variations in phenotypes in the center of lesions share similarities with malignant diseases, in which cells originating from the central part of the primary tumor usually remain in a differentiated state while cells in the outer areas of the primary tumor express an invasive phenotype and aggressive behavior, colonizing the neighborhood and leading to cancer metastasis (17–19). These features are highly indicative of collective cell migration, described for other pathologic and physiologic events (20, 21). This morphologic characteristic may be explained by traction generated during the invasion process. In collective cell migration, cells that remain at the leading edge and establish contacts with the extracellular matrix (ECM) generate traction, guiding the movement of the trailing edge, defined as a group of cells in close contact that follow the movement (22). Partial or complete differentiation of cells has been observed at the leading edge due to interaction with the ECM, particularly by growth factors such as epidermal growth factor, vascular endothelial growth factor, and fibroblast growth factor and their corresponding downstream targets PI3K, Akt, MAPK, and Rho GTPases (22).

Adhesion Molecules

Adhesion molecules are crucial to the collective cell migration process (23). These protein complexes are formed by extracellular interaction of type 1 cadherins (like E-cadherin) that

bind intracellular β -catenin, creating a protein link that attaches two neighboring cells (24). They are expressed throughout the menstrual cycle in the eutopic uterus as well as by endometriotic gland lesions (25, 26). In the present study, we found homogeneous expression of adhesion molecules, with no difference between the center and front of lesions induced after 1 year. During collective cell migration, cellular membrane contacts are retained (20, 27), allowing direct force transmission to cells by coordination of the cytoskeleton that generates movement and maintains cell-cell contacts (28). This may explain why glands originating from the invasion front can be followed along consecutive serial sections and remain histologically connected to the center. It strongly suggests that the presence of adhesion molecules may well be permanent, albeit with some time variation, throughout the entire migration process and probably plays a crucial role in the attachment and arrangement of cells into a glandular conformation.

Nerves and NGF

PGP9.5 was used for nerve fiber staining as a ubiquitous neuronal marker. This membrane protein is a ubiquitin hydrolase and a common marker for neuronal axons and cell bodies from the central and peripheral nervous system. NFD was higher in lesions induced after 1 year than in eutopic endometrium, which was the opposite of what was found in lesions 6 months after induction (13). Moreover, direct comparison between 6-month lesions and 1-year lesions showed a significant increase in NFD with induction over a longer period, suggesting that endometriosis-associated nerves could evolve, as seen in human disease (29). Indeed, deep nodular endometriotic lesions in humans are known to be more innervated than peritoneal and ovarian endometriosis (30). Anaf et al. demonstrated that in patients with pain scores of >7 , the percentage of nerves located within endometriotic lesions was significantly higher than in patients with pain scores of ≤ 7 (6), indicating a possible relationship between pain and NFD. NGF is a neurotropic factor involved in cell growth, differentiation, inflammation, survival of neurons (31), and axonal growth during the regeneration process (32). In our previous studies, overexpression of NGF was detected 6 months after induction (13). This growth factor may therefore be a potent stimulator of nerve fiber genesis or act as a positive chemotaxin for neurons, facilitating their contact with target tissues through interaction with its receptor, as hypothesized by Anaf et al. to occur in humans (33). However, in the present nonhuman animal model, the abundant nerve fibers observed in lesions after 1 year may possibly originate from the lesion itself or the surrounding area.

After binding to its receptor, NGF can trigger focalized protein synthesis in the injured axonal region, generating synthesis of β -actin required for elongation of nerves (34). It was also reported to be involved in endometriosis development. Gori et al. reported the highest NGF mRNA expression in deep nodular endometriosis and endometriomas, significantly higher than in eutopic endometrium from endometriosis patients and healthy subjects (35). In the

same paper, the authors reported that an in vitro study highlighted NGF induction in response to tumor necrosis factor α treatment. In that study, expression of NGF in endometrial cells was similar between healthy control subjects and endometriosis patients. Our results on NGF expression in eutopic endometrium of baboons and induced lesions indicate that it could also be cyclical, suggesting a potential influence of the environment. Association with inflammation and peripheral nerves is mediated through cytokines and growth factors. In a recent review, the role of mast cells (MCs) was emphasized in the pathogenesis of endometriosis, because both invasion and degranulation of MCs have been widely documented in endometriotic lesions in animal models and humans (36). Chen et al. reported that specific small interfering RNA-mediated silencing of β -NGF gene expression after gene transfer in a rat model with surgically induced endometriosis suppressed growth of ectopic endometriotic implants, resulting in a significant improvement in generalized hyperalgesia, as well as reduced sympathetic and sensory nerve fiber density (37). However, other authors found significantly higher NGF expression in peritoneal endometriosis compared with nonbowel deep infiltrating endometriosis and bowel endometriosis (38). Dewanto et al. reported that endometriotic lesions express the neurotrophins brain-derived neurotropic factor and NGF and their receptors TrkA, TrkB, and p75. They postulated an autocrine function in endometriosis, although a clear causative picture did not emerge, owing to the redundancy and complexity of the signaling system. We, like others before us (33,39–42), showed that NGF is expressed in both endometrium and endometriotic lesions, but at higher levels in deep nodular endometriosis (31). Peritoneal fluid from women with endometriosis was also found to contain high levels of NGF (43, 44), confirming that neurotrophin overexpression is not triggered by eutopic endometrium, but directly by endometriotic lesions and their environment. This growth factor could therefore be a potent stimulator of nerve fiber genesis in endometriotic lesions themselves, with higher levels of NGF expression in deep infiltrating lesions inducing a greater density of nerve fibers. As hypothesized by Anaf et al. (33), NGF could act as a positive chemotaxin for neurons and may therefore facilitate their contact with target tissues through interaction with its receptors, explaining why deep nodular lesions essentially occur in richly innervated anatomic sites (such as the rectovaginal septum and uterosacral ligaments).

In the present study, NGF values in 12-month lesions differ from values in 6-month lesions, which are significantly higher than in their corresponding eutopic endometrium. Taking into account the grafting procedure used in our model, it may be possible that NGF is involved in the survival of neurons already present in grafted tissue (eutopic endometrium and myometrium, ie, the JZ), as well as in recruitment of nerves from neighboring tissue by means of axonal guidance. Increased NFD and decreased NGF expression after 1 year suggest that during the first 6 months, inflammation and hypoxia could result in loss of nerve fibers, which may then trigger an increase in NGF to promote nerve fiber recruitment, in turn leading to higher NFD.

CONCLUSION

This is the first study to analyze the kinetic evolution of deep nodular endometriotic lesions induced in an animal model. Nodular endometriotic lesions induced over the course of 1 year in the baboon model showed a 100% invasive phenotype, with significantly reduced glandular thickness, significantly higher mitotic activity, and stable adhesion molecules, compared with 6-month nodular endometriotic lesions. In addition, NFD was significantly increased in these 1-year lesions and NGF expression significantly decreased. These changes are highly indicative of collective cell migration and not only persist beyond 12 months, but also appear to increase with time concomitantly with NFD. Our study strongly suggests that nerve fibers play a role in the development of lesions, as observed in women, but further studies are needed to pinpoint the origin of these nerve fibers.

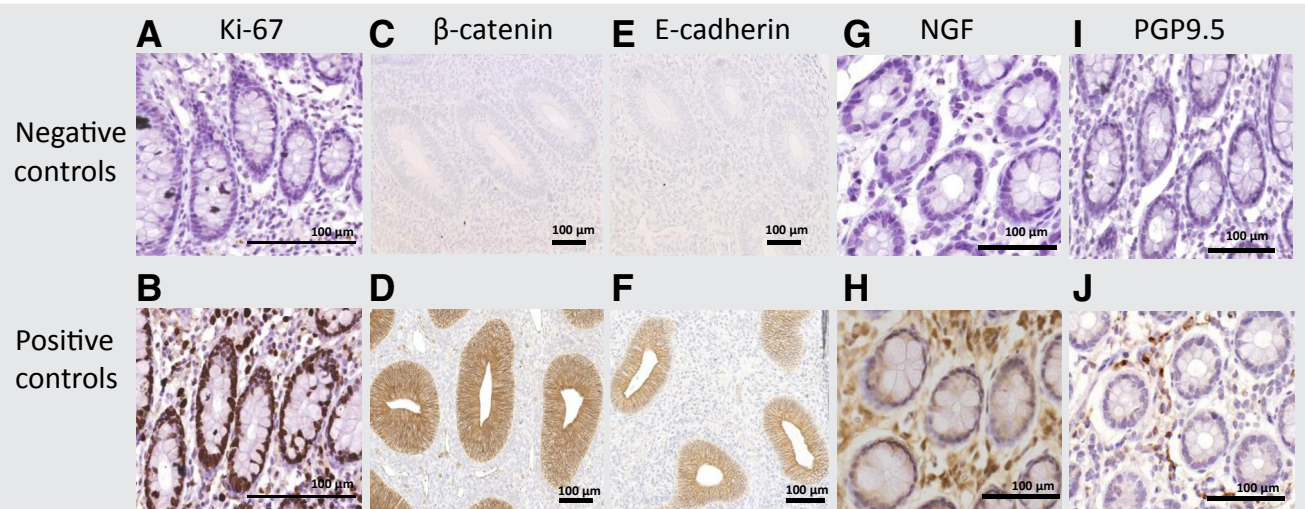
Acknowledgments: The authors thank Mira Hryniuk, B.A., for reviewing the English language of the manuscript.

REFERENCES

1. Wheeler JM. Epidemiology of endometriosis-associated infertility. *J Reprod Med* 1989;34:41–6.
2. Giudice LC, Kao LC. Endometriosis. *Lancet* 2004;364:1789–99.
3. Nisolle M, Donnez J. Peritoneal endometriosis, ovarian endometriosis, and adenomyotic nodules of the rectovaginal septum are three different entities. *Fertil Steril* 1997;68:585–96.
4. Donnez J, Squifflet J. Complications, pregnancy and recurrence in a prospective series of 500 patients operated on by the shaving technique for deep rectovaginal endometriotic nodules. *Hum Reprod* 2010;25:1949–58.
5. Donnez J, Jadoul P, Colette S, Luyckx M, Squifflet J, Donnez O. Deep rectovaginal endometriotic nodules: perioperative complications from a series of 3,298 patients operated on by the shaving technique. *Gynecol Surg* 2013;10:31–40.
6. Anaf V, Simon P, el Nakadi I, Fayt I, Buxant F, Simonart T, et al. Relationship between endometriotic foci and nerves in rectovaginal endometriotic nodules. *Hum Reprod* 2000;15:1744–50.
7. d'Hooghe TM, Bambra CS, Cornillie FJ, Isahakia M, Koninckx PR. Prevalence and laparoscopic appearance of spontaneous endometriosis in the baboon (*Papio anubis*, *Papio cynocephalus*). *Biol Reprod* 1991;45:411–6.
8. d'Hooghe TM, Bambra CS, Suleman MA, Dunselman GA, Evers HL, Koninckx PR. Development of a model of retrograde menstruation in baboons (*Papio anubis*). *Fertil Steril* 1994;62:635–8.
9. Dehoux JP, Defrère S, Squifflet J, Donnez O, Polet R, Mestdagt M, et al. Is the baboon model appropriate for endometriosis studies? *Fertil Steril* 2011;96:728–33.
10. Donnez O, Jadoul P, Squifflet J, Donnez J. Iatrogenic peritoneal adenomyoma after laparoscopic subtotal hysterectomy and uterine morcellation. *Fertil Steril* 2006;86:98–101.
11. Donnez O, Squifflet J, Leconte I, Jadoul P, Donnez J. Posthysterectomy adenomyotic masses observed in 8 cases out a series of 1405 laparoscopic subtotal hysterectomies. *J Minim Invasive Gynecol* 2007;14:156–60.
12. Donnez O, van Langendonck A, Defrère S, Colette S, van Kerk O, Dehoux JP, et al. Induction of endometriotic nodules in an experimental baboon model mimicking human deep nodular lesions. *Fertil Steril* 2013;99:783–9.
13. Donnez O, Soares M, Defrère S, Dehoux JP, van Langendonck A, Donnez J, et al. Nerve fiber density in deep nodular endometriotic lesions induced in a baboon experimental model. *Fertil Steril* 2013;100:1144–50.
14. Donnez O, Orellana R, Van Kerk O, Dehoux JP, Donnez J, Dolmans MM. Invasion process of induced deep nodular endometriosis in an experimental baboon model: similarities with collective cell migration? *Fertil Steril* 2015;104:491–7.
15. Koninckx P, Ussia A, Adamyan L, Wattiez A, Donnez J. Deep endometriosis: definition, diagnosis, and treatment. *Fertil Steril* 2012;98:564–71.
16. Abbot J.A. Adenomyosis and abnormal uterine bleeding (AUB-A)—pathogenesis, diagnosis, and management. *Best Pract Res Clin Obstet Gynaecol*. 2016 Sep 30. pii: S1521-6934(16)30083-9. [Epub ahead of print.]
17. Brabletz T, Jung A, Reu S, Porzner M, Hlubek F, Kunz-Schughart LA, et al. Variable beta-catenin expression in colorectal cancers indicates tumor progression driven by the tumor environment. *Proc Natl Acad Sci U S A* 2001;98:10356–61.
18. Cao C, Chen Y, Masood R, Sinha UK, Kobiela A. α -Catulin marks the invasion front of squamous cell carcinoma and is important for tumor cell metastasis. *Mol Cancer Res* 2012;10:892–903.
19. Lv ZD, Kong B, Li JG, Qu HL, Wang XG, Cao WH, et al. Transforming growth factor-beta 1 enhances the invasiveness of breast cancer cells by inducing a Smad2-dependent epithelial-to-mesenchymal transition. *Oncol Rep* 2013;29:219–25.
20. Friedl P, Locker J, Sahai E, Segall JE. Classifying collective cancer cell invasion. *Nat Cell Biol* 2012;14:777–83.
21. Friedl P, Gilmour D. Collective cell migration in morphogenesis, regeneration and cancer. *Nat Rev Mol Cell Biol* 2009;10:445–57.
22. Khalil A, Friedl P. Determinants of leader cells in collective cell migration. *Integr Biol* 2010;2:568–74.
23. Goodwin M, Yap AS. Classical cadherin adhesion molecules: coordinating cell adhesion, signaling and the cytoskeleton. *J Mol Histol* 2004;35:839–44.
24. Poncelet C, Leblanc M, Walker-Combrouze F, Soriano D, Feldmann G, Madelenat P, et al. Expression of cadherins and CD44 isoforms in human endometrium and peritoneal endometriosis. *Acta Obstet Gynecol Scand* 2002;81:195–203.
25. van Patten K, Parkash V, Jain D. Cadherin expression in gastrointestinal tract endometriosis: possible role in deep tissue invasion and development of malignancy. *Mod Pathol* 2010;23:38–44.
26. Rorth P. Collective cell migration. *Annu Rev Cell Dev Biol* 2009;25:407–29.
27. Ewald AJ, Brenot A, Duong M, Chan BS, Werb Z. Collective epithelial migration and cell rearrangements drive mammary branching morphogenesis. *Dev Cell* 2008;14:570–81.
28. Matsuzaki S, Darcha C. Epithelial to mesenchymal transition-like and mesenchymal to epithelial transition-like processes might be involved in the pathogenesis of pelvic endometriosis. *Hum Reprod* 2012;27:712–21.
29. Anaf V, Chapron C, el Nakadi I, de Moor V, Simonart T, Noël JC. Pain, mast cells, and nerves in peritoneal, ovarian, and deep infiltrating endometriosis. *Fertil Steril* 2006;86:1336–43.
30. Donnez O, Soares M, Defrère S, van Kerk O, van Langendonck A, Donnez J, et al. Nerve fibers are absent in disease-free and eutopic endometrium, but present in endometriotic (especially deep) lesions. *J End Pelvic Pain Disorders* 2013;5:68–76.
31. Marín O, Valiente M, Ge X, Tsai LH. Guiding neuronal cell migrations. *Cold Spring Harb Perspect Biol* 2010;2:a001834.
32. Willis DE, van Niekerk EA, Sasaki Y, Mesngon M, Merianda TT, Williams GG, et al. Extracellular stimuli regulate localized levels of individual neuronal mRNAs. *J Cell Biol* 2007;178:965–80.
33. Anaf V, Simon P, el Nakadi I, Fayt I, Simonart T, Buxant F, et al. Hyperalgesia, nerve infiltration and nerve growth factor expression in deep adenomyotic nodules, peritoneal and ovarian endometriosis. *Hum Reprod* 2002;17:1895–900.
34. Huang E, Reichardt L. Neurotrophins: roles in neuronal development and function. *Annu Rev Neurosci* 2001;24:677–736.
35. Gori M, Luddi A, Belmonte G, Piomboni P, Tosti C, Funghi L, et al. Expression of microtubule associated protein 2 and synaptophysin in endometrium: high levels in deep infiltrating endometriosis lesions. *Fertil Steril* 2016;105:435–43.
36. Donnez J, Binda MM, Donnez O, Dolmans MM. Oxidative stress in the pelvic cavity and its role in the pathogenesis of endometriosis. *Fertil Steril* 2016;106:1011–7.
37. Chen Y, Li D, Zhang Z, Takushige N, Kong BH, Wang GY. Effect of siRNA against β -NGF on nerve fibers of a rat model with endometriosis. *Reprod Sci* 2014;21:329–39.
38. Dewanto A, Dudas J, Glueckert R, Mechsner S, Schrott-Fischer A, Wildt L, et al. Localization of TrkB and p75 receptors in peritoneal and deep

- infiltrating endometriosis: an immunohistochemical study. *Reprod Biol Endocrinol* 2016;14:43–56.
39. Wang G, Tokushige N, Russell P, Dubinovsky S, Markham R, Fraser IS. Hyperinnervation in intestinal deep infiltrating endometriosis. *J Minim Invasive Gynecol* 2009;16:713–9.
 40. Arnold J, Barcena de Arellano ML, Rüster C, Vercellino GF, Chiantera V, Schneider A, Mechsner S. Imbalance between sympathetic and sensory innervation in peritoneal endometriosis. *Brain Behav Immun* 2012;26:132–41.
 41. Tokushige N, Markham R, Russell P, Fraser IS. Effects of hormonal treatment on nerve fibers in endometrium and myometrium in women with endometriosis. *Fertil Steril* 2008;90:1589–98.
 42. Mechsner S, Schwarz J, Thode J, Loddenkemper C, Salomon DS, Ebert AD. Growth-associated protein 43–positive sensory nerve fibers accompanied by immature vessels are located in or near peritoneal endometriotic lesions. *Fertil Steril* 2007;88:581–7.
 43. Barcena de Arellano ML, Arnold J, Vercellino F, Chiantera V, Schneider A, Mechsner S. Overexpression of nerve growth factor in peritoneal fluid from women with endometriosis may promote neurite outgrowth in endometriotic lesions. *Fertil Steril* 2011;95:1123–6.
 44. Barcena de Arellano ML, Arnold J, Vercellino GF, Chiantera V, Ebert AD, Schneider A, Mechsner S. Influence of nerve growth factor in endometriosis-associated symptoms. *Reprod Sci* 2011;18:1202–10.

SUPPLEMENTAL FIGURE 1



Photomicrograph illustrating positive and negative controls for immunohistochemistry. Ki67 immunostaining of the bowel mucosa (A) without the primary antibody and (B) with anti-Ki67 antibody. β -Catenin and E-cadherin immunostaining of endometrial glands (C, E) in the presence of and (D, F) in the absence of the primary antibody with anti- β -catenin and anti-E-cadherin antibodies. Protein gene product (PGP) 9.5 and nerve growth factor (NGF) immunostaining of the bowel mucosa (G, I) without primary antibody and (H, J) with anti-NGF and anti-PGP9.5.

Orellana. Endometriosis: innervation and invasion. *Fertil Steril* 2017.

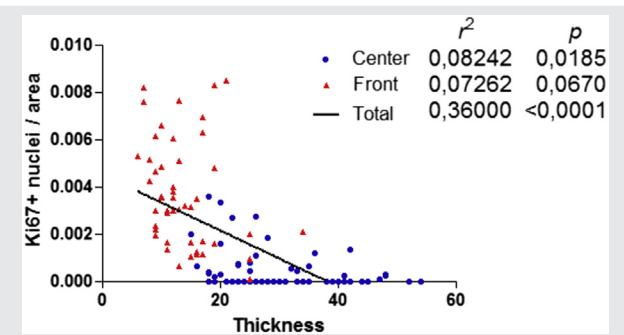
SUPPLEMENTAL FIGURE 2

	6 months*	1 year
Endometriosis (%)	100	100
Volume (mm ³)	415 ± 741.60	531.15 ± 389.28
Surface (mm ²)	29.60 ± 48.60	32.50 ± 21.81
Glandular density (/mm ²)	4.90 ± 5.29	2.48 ± 2.05
Invasion (%)	42.29	100

Morphologic analysis of lesions (n = 15). Values are expressed as mean ± SD. *Adapted from Donnez et al. (12).

Orellana. Endometriosis: innervation and invasion. *Fertil Steril* 2017.

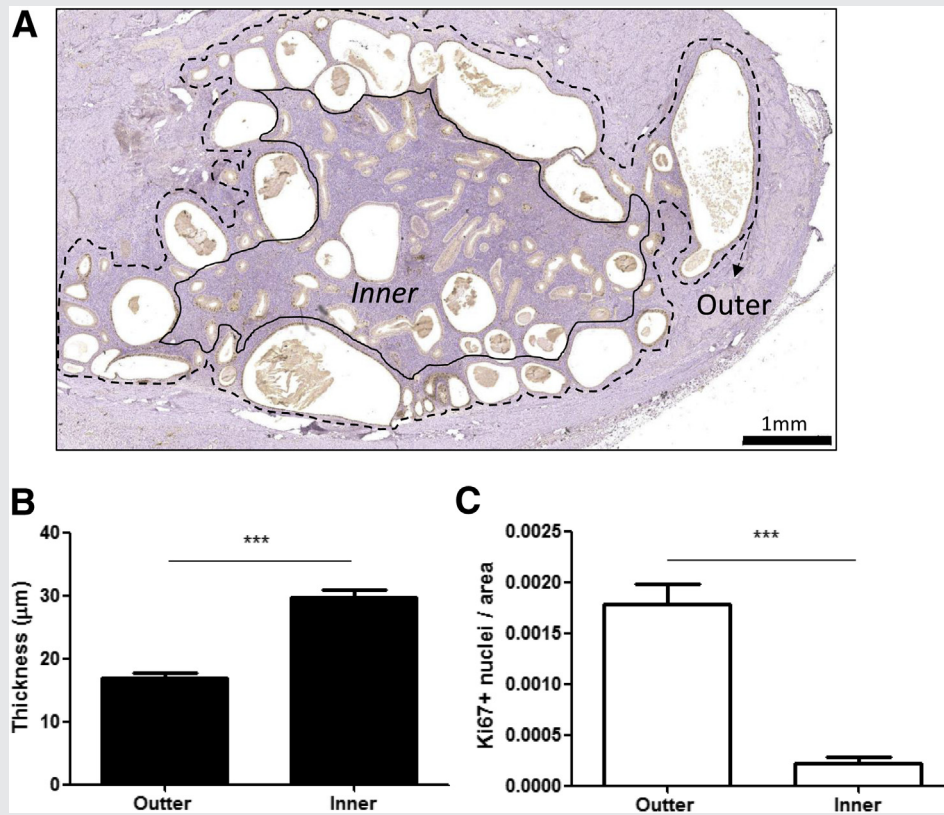
SUPPLEMENTAL FIGURE 3



Correlation between gland thickness and mitotic activity. Graphic representation of linear regression analysis, showing a significant correlation for total glands ($n = 74$; $P < .001$) and central areas ($n = 49$; $P = .0185$), indicating that the thinner the glands, the higher the mitotic activity.

Orellana. Endometriosis: innervation and invasion. Fertil Steril 2017.

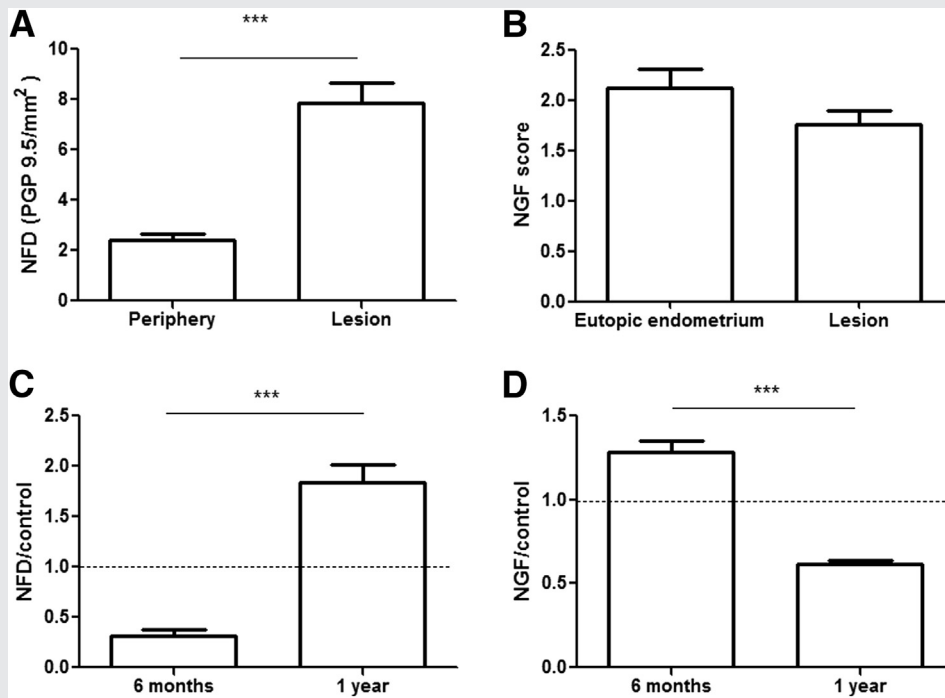
SUPPLEMENTAL FIGURE 4



Analysis of the center of invasive lesions. (A) Distinction between "outer" (dotted black line) and "inner" (continuous black line) glands from the center of lesions. (B) Statistical analysis of gland thickness. Outer glands ($n = 45$) were significantly thinner than inner glands ($n = 44$). $***P < .001$. (C) Mitotic activity analysis. Ki67 showed significantly higher expression in outer glands ($n = 68$) than inner glands ($n = 88$). $***P < .001$. Taken together, these observations suggest possible acquisition of an invasive phenotype over time, which could cause these glands to migrate out of the center and subsequently become part of the invasion front.

Orellana. Endometriosis: innervation and invasion. *Fertil Steril* 2017.

SUPPLEMENTAL FIGURE 5



Comparative analysis of nerve growth factor (NGF) and protein gene product (PGP) 9.5 levels. **(A)** PGP9.5 analysis. Peripheral areas ($n = 12$) revealed significantly higher nerve fiber density (NFD) than lesion areas ($n = 12$). $***P < .001$. **(B)** NGF expression in stromal cells. No significant difference was found between the eutopic endometrium group ($n = 3$) and the lesion group ($n = 13$); $P = .178$. **(C)** PGP9.5 analysis of 6-month ($n = 28$; adapted from Donnez et al. [13]) and 1-year ($n = 12$) lesions. Data were normalized with the use of corresponding eutopic endometrium values (dotted line). NFD was significantly greater in lesions induced over 12 months than 6 months. $***P < .001$. **(D)** NGF expression in glands in 6-month ($n = 18$, adapted from Donnez et al. 2013 [13]) and 1-year ($n = 15$) lesions. Data were normalized with the use of corresponding eutopic endometrium values (dotted line). NGF expression was significantly higher in lesions induced after 6 months than after 1 year. $***P < .001$.

Orellana. Endometriosis: innervation and invasion. *Fertil Steril* 2017.